

Recent data by Murdock and McHargue²⁴ on the diffusion of Ti⁴⁴ in vanadium and a series of vanadium-titanium alloys, ranging from 10 at.% titanium in vanadium to 10 at.% vanadium in titanium in steps of 10 at.% titanium, show that the temperature dependence of diffusion varies continuously with composition from the sharp change of slope in the $\log D$ versus $1/T$ plot in pure vanadium to a continuously curving plot

²⁴ J. F. Murdock and C. J. McHargue, *Acta Met.* **16**, 493 (1968).

for titanium. Thus, it can be inferred that two mechanisms of diffusion also operate in titanium and possibly in all of the anomalous metals.

ACKNOWLEDGMENTS

The authors are indebted to Professor David Lazarus for the use of his laboratories and for his guidance. Thanks are due S. J. Rothman for his suggestions on the solvent extraction methods, and to Dr. D. Gupta for many helpful discussions.

Band Structure and Electronic Properties of Silver

P. E. LEWIS AND P. M. LEE

Physics Department, University of Lancaster, Bailrigg, Lancaster, England

(Received 29 April 1968; revised manuscript received 15 July 1968)

A band-structure calculation for silver has been made using Mueller's interpolation scheme. The first-principles calculation by Segall has been adjusted to give better agreement with experiment, and a set of parameters derived to fit these adjusted bands. A density-of-states calculation using these parameters confirms deductions from experimental work using the photoelectric effect which suggest two main peaks in the *d*-band region. However, we find an additional low-energy peak which has not been observed experimentally and no evidence of structure near the Fermi level. The Fermi surface is computed after a recalculation of the Fermi energy which agrees with Segall's results. Reasonable correlation with the experimental dimensions of the Fermi surface is obtained. Finally, various effective masses are calculated. The value obtained for the electronic specific heat suggests that electron-phonon enhancement is somewhat smaller in silver than in copper.

1. INTRODUCTION

SEVERAL interpolation schemes have been constructed in recent years in an attempt to describe the energy bands of noble and transition metals.¹⁻³ That by Mueller³ seems to be the most plausible physically and can actually be derived, subject to various approximations, from the Green's functions (or KKR⁴) theory of energy bands.⁵⁻⁷

The important point about an interpolation scheme is that from a relatively small amount of data—perhaps a first-principles calculation of eigenvalues at symmetry points in the Brillouin zone, or, alternatively, an experimentally determined Fermi surface—one can derive parameters for use in the interpolation scheme and then use these same parameters to extend the results to any part of the Brillouin zone. This process greatly facilitates calculation of such quantities as the electronic density of states, effective masses, etc. General considerations as to the philosophy of using

such interpolation schemes have been discussed by Phillips.⁸

In this paper we describe how a one-electron band structure for silver has been obtained and show that this structure will predict various electronic quantities in reasonable agreement with experiment. The work described is a preliminary to studies of noble-transition-metal alloys, in particular those of the silver-palladium series.

2. CALCULATED SILVER BAND STRUCTURE

A. Previous Band Calculations

The only first-principles calculation for silver appears to be that due to Segall.⁹ For reasons explained in his paper Segall did not claim great accuracy and, indeed, although the general shape of his bands are in qualitative agreement with those of the similar metal copper (except that in silver the *d* bands are derived from the 4*d*, rather than the 3*d*, atomic levels), some of the more quantitative features of the bands are plainly incorrect. In particular, in neither of his calculations, using two different potentials, was Segall able to predict the height of the *d* bands relative to the conduction bands so as to agree with the (admittedly tentative) interpretation of optical data. These data would place the

¹ M. Saffren, in *The Fermi Surface*, edited by W. A. Harrison (John Wiley & Sons, Inc., New York, 1960), p. 341.

² L. Hodges, H. Ehrenreich, and N. D. Lang, *Phys. Rev.* **152**, 505 (1966).

³ F. M. Mueller, *Phys. Rev.* **153**, 659 (1967).

⁴ W. Kohn and N. Rostoker, *Phys. Rev.* **94**, 1111 (1954).

⁵ J. M. Ziman, *Proc. Phys. Soc. (London)* **86**, 337 (1965).

⁶ V. Heine, *Phys. Rev.* **153**, 673 (1967).

⁷ R. Jacobs, *Proc. Phys. Soc. (London)*, Ser. 2, **1**, 492 (1968).

⁸ J. C. Phillips, *Advan. Phys.* **17**, 79 (1968).

⁹ B. Segall, G.E. Research Report No. 61-RL-(2785G), 1961 (unpublished).

Fermi level about 4 eV above the d bands, whereas, when using a potential derived from the Hartree free-ion-core functions, Segall found the d bands to be 2.2 eV below E_F and a value for the neck radius of the Fermi surface which was much larger than that found experimentally; when using Hartree-Fock functions to derive a potential, the d bands were too low (5.2 eV below E_F), while the Fermi surface was found to be much more spherical and not in contact with the zone boundary at all.

It was suggested by Segall that a rigid shift of the d bands to the "correct" level, i.e., the one predicted from optical data, would also predict the experimental Fermi surface because the hybridization interactions between the d and conduction bands would then be of the right order of magnitude. Basically, we have carried out Segall's suggestion in that we have adjusted the d bands relative to the conduction bands so as to agree with various experimental work which we now discuss, and then show that the Fermi surface which we calculate does indeed have similar dimensions to that found experimentally. This is not perhaps very surprising, but it is satisfying to correlate results from different experimental phenomena (de Haas-van Alphen effect, magnetoresistance, optical properties) with an abstract interpolation scheme and a first-principles band calculation.

B. Experimental Data

Relevant experimental work as far as the silver band structure is concerned is the work on optical properties by Ehrenreich and Philipp¹⁰ and photoelectric measurements by Berglund and Spicer.¹¹

The simplest ideas are by Ehrenreich *et al.*, who assume that the imaginary part ϵ_2 of the dielectric constant between 4 and 10 eV is due to specific inter-band transitions, or to transitions to or from the Fermi level. Since the probability that such transitions will occur depends on the densities of states of the bands taking part, and these are largest at symmetry points, these authors relate the structure in ϵ_2 to specific gaps at symmetry points. They appeal to the similar structure of copper when in doubt as to which gap corresponds to which peak in ϵ_2 .

This approach can, and has, been criticized on several grounds, e.g., it assumes that the one-electron band structure is literally true, that only vertical (i.e., \mathbf{k} -conserving) transitions are possible, and it takes no account of variations in oscillator strengths for such transitions. We do not here further discuss the validity of Ehrenreich's approach, since this has been done by several authors, e.g., Phillips¹²; we merely quote their result, which is that if Segall's calculated band structure, using a Hartree free-ion function, has the d bands

TABLE I. Comparison of the data from optical and photoelectric work on energy gaps at symmetry points in the silver Brillouin zone.

Gap	Optical data ^a		Photoelectric		Actual fit (Ry)
	(eV)	(Ry)	(eV)	(Ry)	
F.S. \rightarrow X_4'	1.7 ^b	0.12	1.8 ^c	0.13	0.14
$X_5 \rightarrow X_4'$	5.4 ^d	0.40	5.55	0.41	0.44
$X_5 \rightarrow$ F.S.	3.7 ^b	0.27	3.75	0.28	0.30
$X_1 \rightarrow X_4'$	9.1 ^d	0.67			0.68
$X_1 \rightarrow X_5$ (d bandwidth)	3.7 ^d	0.27	3.5	0.26	0.23
$L_2' \rightarrow L_1$	6.0 ^d	0.44	4.2	0.31	0.34
$L_2' \rightarrow$ F.S.		0.03	0.3	0.02	0.03
F.S. $\rightarrow L_1$			3.9	0.29	0.31
$L_3 \rightarrow$ F.S.	3.9 ^d	0.29			0.32
$W_1 \rightarrow W_3$	9.8 ^d	0.72			0.77

^a Here we have followed Ehrenreich and Philipp in shifting the d bands down through 1.8 eV and also the level L_2' . The actual values have been estimated from the graph in Segall (Ref. 9).

^b Rigid shift of d bands of Segall (Ref. 9) down through 1.8 eV.

^c Probable value (Ref. 11).

^d Estimated from graph or deduced from it.

shifted rigidly down through 1.8 eV, then the shape of ϵ_2 can be explained.

The photoelectric work of Berglund and Spicer¹¹ is useful in that it, too, enables us, with perhaps rather more confidence than in the case of the optical work, to deduce band gaps at symmetry points. (It also produces a density-of-states curve, but we defer consideration of this until Sec. 3.) Another result of this work is that it can be explained by assuming that transitions between energy levels are non-direct in most cases, i.e., crystal momentum \mathbf{k} is not conserved. This is one of the main reasons for doubting the Ehrenreich approach.

So far as we are concerned at present, though, in trying to deduce a reasonable one-electron picture for silver, the differences between the two approaches do not appear to be too important. In Table I we summarize the evidence on the silver band gaps deduced from the two methods; it is seen that with one exception (*viz.*, the band gap $L_2' - L_1$) the different approaches do not produce badly conflicting evidence. The discrepancy at L would be explained by the fact that all the other levels which Ehrenreich has shifted down are d levels, whereas the level L_2' is a p level. Hence we reject this shifting of L_2' and just rigidly shift the d levels.

C. Parameters and Final Band Structure

We list in Table II the final eigenvalues (relative to the bottom Γ_1 of the conduction band) at the symmetry points Γ , X , L , and W , which we have attempted to fit. We also show the best fit we have obtained using the set of parameters listed in Table III, which is the best set we have been able to obtain. (We do not discuss here the actual process of fitting the bands.)

It can be seen that a reasonable, if by no means perfect, fit has been obtained—the rms deviation being 0.016 Ry. This figure is admittedly not as good as that of Mueller,³ who obtained a value of 0.006 Ry

¹⁰ H. Ehrenreich and H. R. Philipp, Phys. Rev. **128**, 1622 (1962).

¹¹ C. N. Berglund and W. E. Spicer, Phys. Rev. **136**, A1044 (1964).

¹² J. C. Phillips, Phys. Rev. **140**, A1254 (1965).

TABLE II. List of silver eigenvalues we attempted to fit and the actual fit using the parameters listed in Table III. All values in rydbergs.

Level	Estimated value	Actual fit	Difference
Γ_1	0.0	0.0	0.0
Γ_{25}'	0.141	0.150	-0.009
Γ_{12}	0.215	0.224	-0.009
X_1	0.015	0.033	-0.018
X_3	0.042	0.054	-0.012
X_2	0.268	0.248	0.02
X_5	0.282	0.258	0.024
X_4'	0.687	0.700	-0.013
X_1	1.067	1.071	-0.004
L_1	0.028	0.039	-0.011
L_3	0.141	0.151	-0.01
L_2	0.268	0.242	0.026
L_2'	0.535	0.526	0.014
L_1	0.854	0.864	-0.01
W_2	0.075	0.072	0.003
W_3	0.122	0.143	-0.021
W_1	0.220	0.205	0.015
W_1'	0.282	0.246	0.036
W_3	1.00	1.011	-0.011
rms			0.016

on the same bands in copper. However, it must be remembered that the copper bands which Mueller was fitting were based on much more definite evidence—viz., two first-principles calculations (by different methods but using the same potential) which produced very similar results, rather than on a mixture of a rather uncertain band calculation and various experimental results which, as we have indicated, are by no means capable of a unique interpretation.

It is of interest, in view of the desirability of reducing the number of independent parameters in an interpolation scheme, to compare our derived parameters with Phillips's⁸ recent suggestion that the orthogonality and hybridization interactions (the quantities A , R_0 , B , and R_1 in Table III) actually depend on only one quantity—the width W of the d bands through a factor $W^{1/2}$. We illustrate our results in Table IV, where we have taken the width of the d band to be the difference in energy between the levels X_1 and X_5 . In this we have compared the parameters derived by Mueller to fit the copper calculations of Burdick¹³ and of Segall,¹⁴ i.e.,

TABLE III. Parameters to fit the silver band structure. Notation as in Mueller (Ref. 3).

	Parameter	Value
d bands	d_0	0.179 Ry
	$dd\sigma$	-0.027 Ry
	$dd\pi$	0.016 Ry
	$dd\delta$	-0.003 Ry
Fourier components of potential	V_{111}	0.019 Ry
	V_{200}	0.040 Ry
Orthogonality	A	1.30
	R_0	3.50
Hybridization	B	0.92 Ry
	R_1	3.70

¹³ G. A. Burdick, Phys. Rev. **129**, 138 (1963).

TABLE IV. Comparison of orthogonality and hybridization parameters for two copper calculations (Ref. 3) and the present silver calculation.

Copper B^a Copper S^b	Copper S Silver ^c	Copper B Silver
$W_S^{1/2}/W_B^{1/2}=1.096$	$W_S^{1/2}/W_{Ag}^{1/2}=1.156$	$W_B^{1/2}/W_{Ag}^{1/2}=1.055$
$A_S/A_B^d=1.232$	$A_S/A_{Ag}=1.223$	$A_B/A_{Ag}=0.99$
$R_{0S}/R_{1S}=1.052$	$R_{0S}/R_{0Ag}=1.0$	$R_{0B}/R_{0Ag}=0.95$
$B_S/B_B=1.010$	$B_S/B_{Ag}=1.114$	$B_B/B_{Ag}=1.102$
$R_{1S}/R_{1B}=1.184$	$R_{1S}/R_{1Ag}=1.084$	$R_{1B}/R_{1Ag}=0.92$
rms deviation ^e =0.094	rms deviation =0.095	rms deviation =0.094

^a Parameters for copper calculation of Burdick (Ref. 13).

^b Parameters for copper calculation of Segall (Ref. 14).

^c Parameters for present silver calculation.

^d Notation for all parameters is the same as in Mueller (Ref. 3). The subscripts B and S refer to Burdick and Segal calculations.

^e Deviation from exact proportionality to $W^{1/2}$.

the parameters on which Phillips bases his suggestions, with our own for silver. It is seen that the idea that these interactions are proportional to $W^{1/2}$ is not an unreasonable one and this lends weight to the theory that future calculations can be done using a far smaller number of independent parameters than to date.

In Table V we compare the actual d -band parameters—the two-center overlap integrals. According to the theory of Heine,⁶ the ratios of these integrals should be fixed by the crystal structure, apart from a small energy dependence. It is seen from the table that there is moderate agreement with this theory.

3. DENSITY OF STATES

A. Previous Work

As a first application of having fitted a fairly plausible silver band structure, we have calculated a density-of-states curve for silver. This appears to be the first such curve for silver derived directly from a band structure; the only previous calculation for silver is one based on the photoelectric measurements of Berglund and Spicer.¹¹

The main features of the curve inferred by these writers is the presence of two peaks at energies of about 4 and 5.3 eV, respectively, below the Fermi level. They also find a very small subsidiary peak just below the Fermi level. The actual heights of these peaks are rather uncertain since the interpretation of the experimental results is not entirely unambiguous. It is reasonable to interpret the two large peaks as being due mainly to the high density of states in the d bands,

TABLE V. Comparison of d -band parameters.

Ratio	Copper B	Copper S	Silver
$ dd\sigma/dd\pi ^a$	1.94	1.88	1.66
$ dd\pi/dd\delta $	9.0	6.0	5.33

^a Notation is the same as in Mueller (Ref. 3).

¹⁴ B. Segall, Phys. Rev. **125**, 109 (1962).

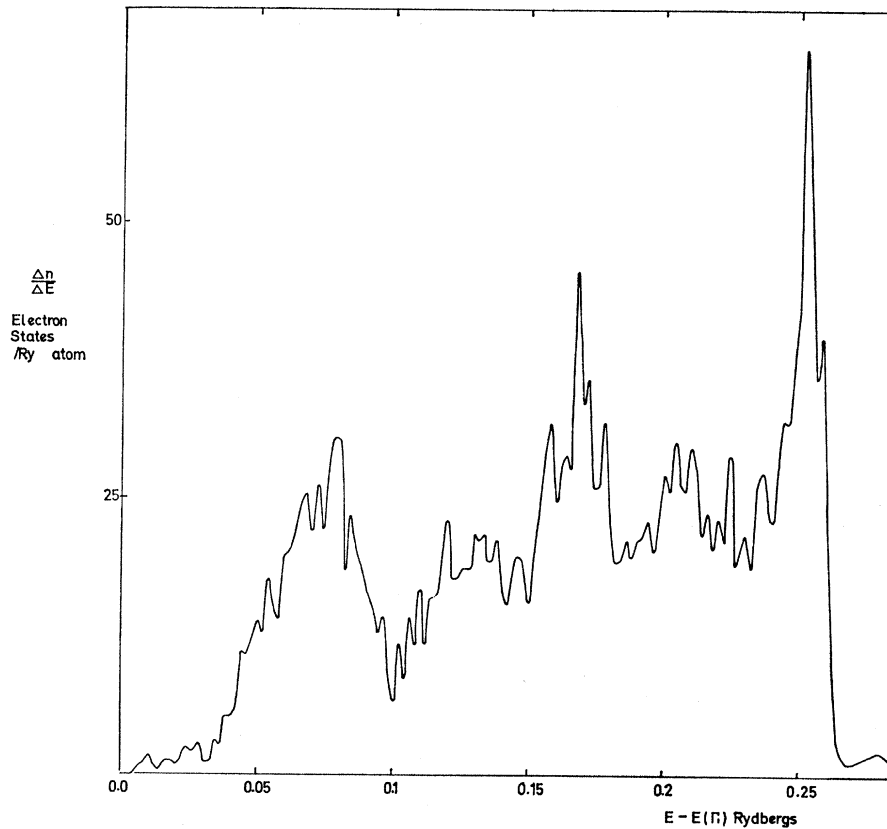


FIG. 1. Lower part of density-of-states curve for silver showing structure due to d bands and conduction bands.

but the explanation of the peak just below E_F is uncertain.

No other structure shows up from the photoelectric work, but the main features provide a useful guide as to the plausibility or otherwise of the present calculation; we expected from the outset, however, that our more direct calculation would show up considerably more structure than the experimentally derived curve.

B. Method

Since E , regarded as a function of \mathbf{k} , has the symmetry of the Brillouin zone, and since this symmetry is cubic for the silver fcc lattice, it is only necessary to compute eigenvalues in any $1/48$ wedge of the zone since all possible eigenvalues will occur in this wedge.

Hence we used a random number generator to give us a selection of points in k space and imposed geometrical conditions to ensure that only points in one particular wedge were used. The generator was thoroughly tested to ensure that the numbers used were truly random and that cycling did not occur during the course of the computation.

As a check for self-consistency, the density of states was calculated twice using different sets of random numbers, and in each case the same essential features were obtained.

C. Results

The calculated density of states for silver is shown in Fig. 1; the curve is based on the lowest six eigenvalues at 2000 randomly generated points in one particular wedge. An energy interval of 0.002 Ry is used.

Our results are in quantitative agreement with the photoelectric curve in that we find two main peaks at -0.3 Ry (-4.1 eV) and -0.39 Ry (-5.3 eV) relative to the Fermi level. (We have calculated the Fermi level independently as will be described later.) The first of these peaks, however, is substantially sharper than that inferred from the experimental work. It should be noted that the energies at which these main peaks occur coincide with the energies at various symmetry points in the zone, though we have not indicated this explicitly in the diagram.

The main difference between our results and those of Berglund and Spicer¹¹ is that we have obtained a fairly large subsidiary peak at -0.48 Ry (-6.54 eV) relative to the Fermi level. Such a peak has been found in copper by Mueller³ in a similar calculation to the present one, i.e., one based on the interpolation scheme, and has also been inferred from the photoelectric work but there appears to be little experimental evidence for its presence in Ag. The peak can be associated with some of the lower energy d bands; it corresponds most closely with the lowest eigenvalue at the symmetry point W .

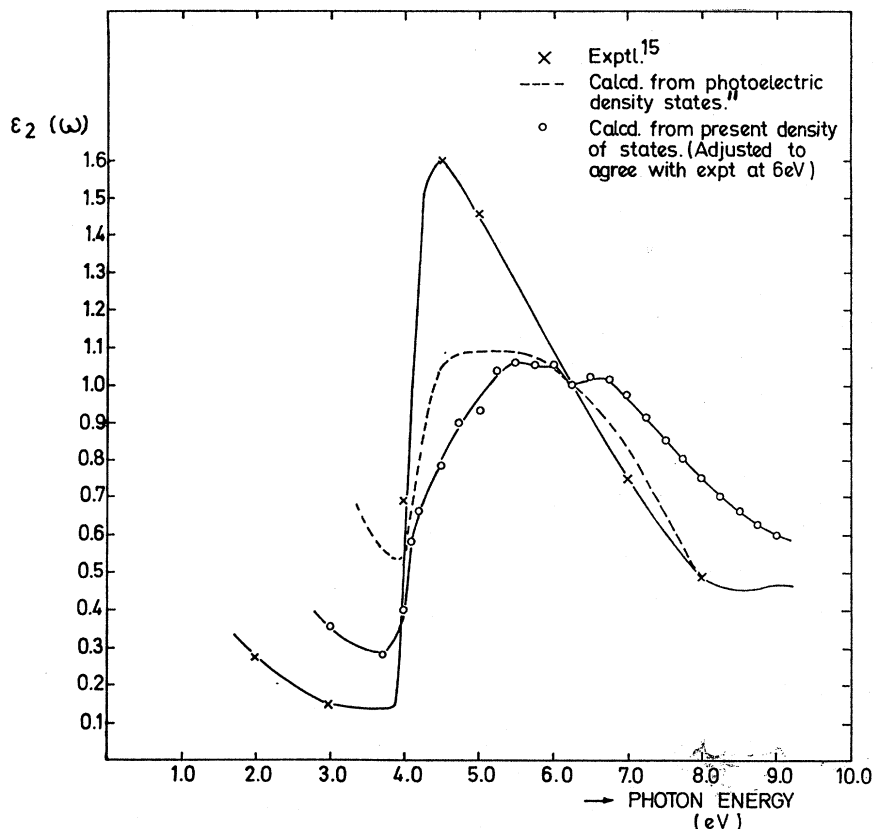


FIG. 2. Imaginary part of silver dielectric current.

If such a peak is physically meaningful, it is perhaps rather curious that it cannot be inferred from any experimental work. [In particular, the low-energy peak in copper shows up as a small shoulder in the imaginary part $\epsilon_2(\omega)$ of the dielectric constant at photon energies of above 6 eV.] The experimental work of Cooper *et al.*¹⁵ shows a small shoulder just below 6 eV but not in the region of 6.5 eV where on simple ideas of interband transitions one would be expected if our low-energy peak is meaningful. On the other hand, closer examination of their results shows that Cooper *et al.* have not got any experimental values between 6 and 7 eV, so it is possible that closer analysis of their results might reveal a small peak or shoulder. Another possibility is that oscillator strengths for transitions from a low-energy peak in the d bands to the Fermi level are small, precluding any experimental confirmation of that peak.

Phillips¹² has suggested that the low-energy peak in copper which was originally postulated to be present in order to explain results of photoelectric work is due to a low-energy many-body resonance. However, a low-energy peak was found at $E - E_F \approx -6$ eV by Mueller in copper using the present interpolation scheme, while we have found an even more prominent one in silver. Since both of these have shown up as a

result of pure band calculations, this would appear to cast doubt on Phillips's interpretation.

This peak showed up in two of our calculations involving different sets of random numbers. We conclude that further experimental analysis is necessary before the question of this low-energy peak can be resolved.

So far as the higher-energy portions of our curve are concerned, we find no definite evidence of any structure above the peaks which we have associated with the d bands. This, of course, might be because we have not used a large enough sample of points in k space, as any possible peaks in this region will be associated with conduction bands and hence are likely, if present at all, to be small.

On the other hand, experimental evidence does tend to support our results. Above the Fermi level Berglund and Spicer¹¹ find no peak in the curve inferred from photoelectric data and suggest that it is this absence which leads to the absence of a second major peak in $\epsilon_2(\omega)$ for silver.¹⁰ [Such a peak does show up in copper, where a small peak in $N(E)$ is found above E_F .] In later work on silver Cooper *et al.*¹⁵ do find a (small) shoulder just below 6 eV which they attribute to a direct transition from the top of the d bands at X_5 to the level X_4' above E_F . This interpretation is of doubtful validity, particularly in view of the uncertainty as to whether such direct transitions do occur, and it is

¹⁵ B. R. Cooper, H. Ehrenreich, and H. R. Philipp, Phys. Rev. 138, A494 (1965).

far from definite evidence of any small peak in $N(E)$ in this region.

Finally, we find no evidence for a small peak about 0.03 eV below E_F such as has been found experimentally. Phillips¹⁶ has suggested on rather tentative grounds that this peak cannot be explained in terms of a one-electron picture but must be attributed to a many-body resonance and our results would tend to support his suggestion.

D. Dielectric Constant of Silver

From our density-of-states curve it is a small extension to actually calculate the variation of the imaginary dielectric constant ϵ_2 with frequency. The calculation is simplified in that it makes various assumptions, e.g., that our one-electron band picture is literally true, that the structure in ϵ_2 is due entirely to interband transitions, and that the probability of a transition from an occupied band to an unoccupied one depends only on the joint density of states. This latter assumption ignores the possible variation over the Brillouin zone of the matrix elements for the transitions.¹⁵

With these assumptions it follows that our variation of ϵ_2 with frequency, which is shown in Fig. 2, is really only an alternative way of displaying the density-of-states curve. Nonetheless, despite the assumptions, the experimental curve between 3 and 9 eV is reproduced fairly well. (We have adjusted the matrix element to produce the best fit to the experimental curve at 6 eV.)

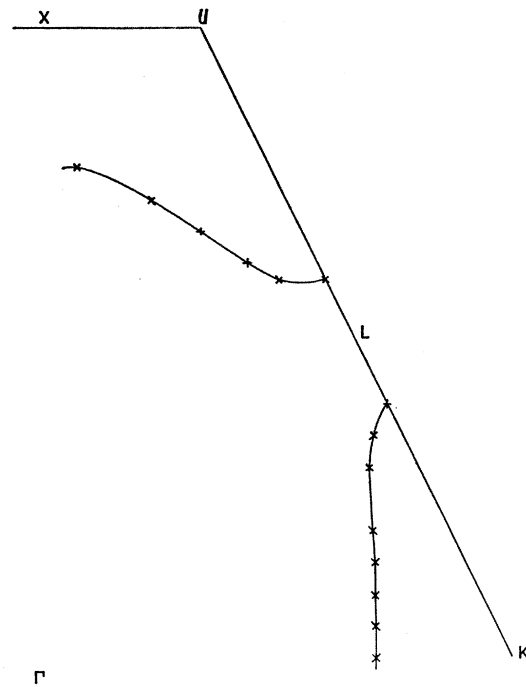
We have discussed experimental work on ϵ_2 in the previous section and merely remark here that the main feature of our results is the subsidiary peak at 6.5 eV. This must be attributed to our low-energy peak in $N(E)$. It does not seem likely that this peak corresponds to the second peak in copper (the origin of which has already been discussed) since it is far closer to the main d -band peak than the corresponding peak in copper, no such peak has shown up experimentally, and the interpretation in terms of the low-energy peak is the most natural in view of the assumptions.

In general, we consider our density-of-states curve to be plausible and proceed to consider another test of our band structure—the surfaces of constant energy, particularly the Fermi surface, that it will predict. We shall further discuss the density-of-states calculation in Sec. 5 when we discuss low-temperature specific heats.

4. FERMI SURFACE OF SILVER

A. Fermi Energy

To determine the Fermi surface in as straightforward a way as possible, we have first of all calculated the Fermi energy E_F ; we have then calculated E_k at various



x indicate calculated points with energies within 0.01 Ry of E_F

FIG. 3. Intersections of (110) plane with surface of constant energy near the Fermi energy.

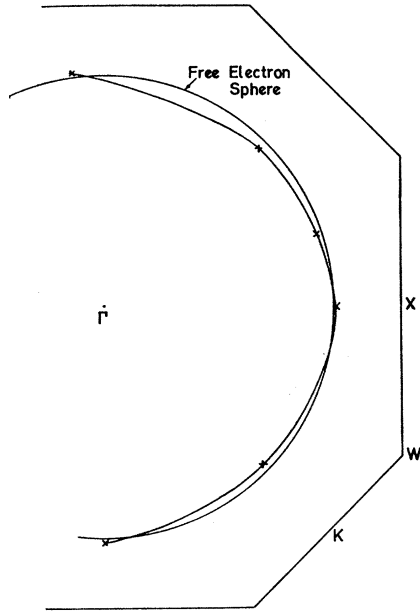
points in the Brillouin zone and found those points k_F which lie on the Fermi surface. Thus we have implicitly solved the equation $E_k = E_F$.

To evaluate the Fermi energy we have followed a procedure which involves calculating eigenvalues at 89 points in the Brillouin zone, these points being equivalent by symmetry to a total of 2048 points.¹³

Each of these 2048 points is at the center of a cubical volume element and it is assumed that the energy in each band at these points is an average for the particular volume in which the point is situated. Then, since each energy band contains two electrons from each atom in the solid, and since we are only interested in bands derived from the $4d$ and $5s$ atomic levels, i.e., a total of 11 electrons per atom in all, it follows that of the eigenvalues at our 2048 points, the first (2048) $(5.5) = 11\,264$ levels will be occupied and the rest unoccupied. Hence, numbering the occupied levels, starting from the lowest, it follows that the level numbered 11 264 is approximately at the Fermi level.

Proceeding in this way for silver, we find that the Fermi level is 0.56 ± 0.01 Ry relative to the bottom Γ_1 of the conduction band. Segall⁹ quotes a value of -0.31 Ry, and since we estimate his value for Γ_1 to be -0.87 Ry, the agreement is good. We have discussed in Sec. 1 how we have adjusted Segall's bands, in particular the d bands, but since the adjusted levels are below the Fermi level, we would not expect appreciable change in this energy.

¹⁶ J. C. Phillips, Phys. Rev. **137**, A1835 (1965).



x Indicate calculated points with energies within 0.01 Ry of E_F

FIG. 4. Intersection of Fermi surface with (100) plane.

B. Fermi Surface

Using this calculated value for E_F , we have plotted constant energy surfaces to give the intersections of the Fermi surface with various planes. We show the intersections with the (110) and (100) planes in Figs. 3 and 4. In the (110) plane we find that the Fermi surface contacts the zone boundary near the center L of the hexagonal face and that the radius of the neck so formed is $0.151 \pm 0.005 r_s$, where r_s is the radius of the free-electron Fermi sphere. This value compares favorably with the experimental values of $0.137 r_s$, using the de Haas-van Alphen effect¹⁷ and $0.142 r_s$, using magnetoresistance.¹⁸ We show in Fig. 5 the variation in Fermi radius in this (110) plane, and compare it with Roaf's experimental results.

In the (100) plane we find comparatively small, though not insignificant deviations, from the free-electron sphere, the surface being pulled out in the $[100]$ direction and pushed in along the $[110]$ direction, the respective radii being $1.01 r_s$ and $0.95 r_s$.

5. EFFECTIVE MASSES IN SILVER

A. Cyclotron Masses

From the calculated Fermi surface of Sec. 4 it is possible to derive information about cyclotron masses for various orbits in silver. It is then instructive to compare the results of this calculation with the experimental results of Roaf¹⁷ and of Howard.¹⁹

¹⁷ D. Shoenberg and D. J. Roaf, Phil. Trans. Roy. Soc. London **255**, 85 (1962).

¹⁸ V. J. Easterling and H. V. Bohm, Phys. Rev. **125**, 812 (1962).

¹⁹ D. G. Howard, Phys. Rev. **140**, 1705 (1965).

It is well known (see, e.g., Ziman²⁰) that the effect of a magnetic field H on an electron at the Fermi surface is to change its k vector in such a way that its energy will be unchanged and it will describe an orbit which is defined by the intersection of the Fermi surface with a plane normal to H . Then, assuming it is not scattered, the electron will complete a circuit in a time

$$\tau = \frac{2\pi}{\omega_H} = \frac{c\hbar}{eH} \oint \frac{dk}{v}$$

on assuming a Lorentz force on the electron. For free electrons where $E \propto k^2$ it is easy to show that $\omega_H = eH/m_0c$, while for electrons which are not free a cyclotron effective mass is defined by

$$\omega_H = eH/m_e^*c$$

and m_e^* varies from orbit to orbit. It can further be shown that

$$m_e^* = \frac{1}{2\pi} \frac{\partial A}{\partial E} \quad (5.1)$$

in atomic units, where A is the area enclosed by the orbit in the plane normal to H .

From the interpolation scheme we have computed the energy contours for various cross sections in the Brillouin zone and can thus approximate the $\partial A/\partial E$ term in (5.1) for various orbits by evaluating the area in k space between neighboring constant energy surfaces. We have done this to obtain m_e^* for three of the principal orbits—the “dog’s bone” orbit from the contours in the (110) plane, the “belly orbit” from the contours in the (100) plane, and the “neck” orbit from the contours on the hexagonal face. These orbits are shown in Fig. 6 and results for the effective masses in Table VI, where they are compared with the experimental data.

It can be seen that fair agreement is obtained with experiment, though the values from the present calculation are, with the exception of the belly orbit, lower by factors probably too large to be accounted for on the basis of experimental or computational errors. It

TABLE VI. Effective masses and areas for various orbits in silver.

Orbit	Effective mass (units of m_0)		Area (units of 10^{16} cm^{-2})	
	Present work	Experiment	Present work	Experiment ^a
“Dog’s bone”	0.91 ± 0.05	1.03 ± 0.01^b	2.0 ± 0.06	1.93
“Neck”	0.21 ± 0.04	0.27 ± 0.03^b 0.35 ± 0.01^c 0.39^d	0.1 ± 0.003	0.095
“Belly”	0.96 ± 0.08	0.94 ± 0.01^b	4.4 ± 0.1	4.8

^a Reference 21.

^b Reference 20.

^c Reference 17.

^d A. S. Joseph and A. C. Thorsen, Phys. Rev. **138**, A1159 (1965).

²⁰ J. M. Ziman, *Principles of the Theory of Solids* (Cambridge University Press, Cambridge, 1965), Chap. 9.

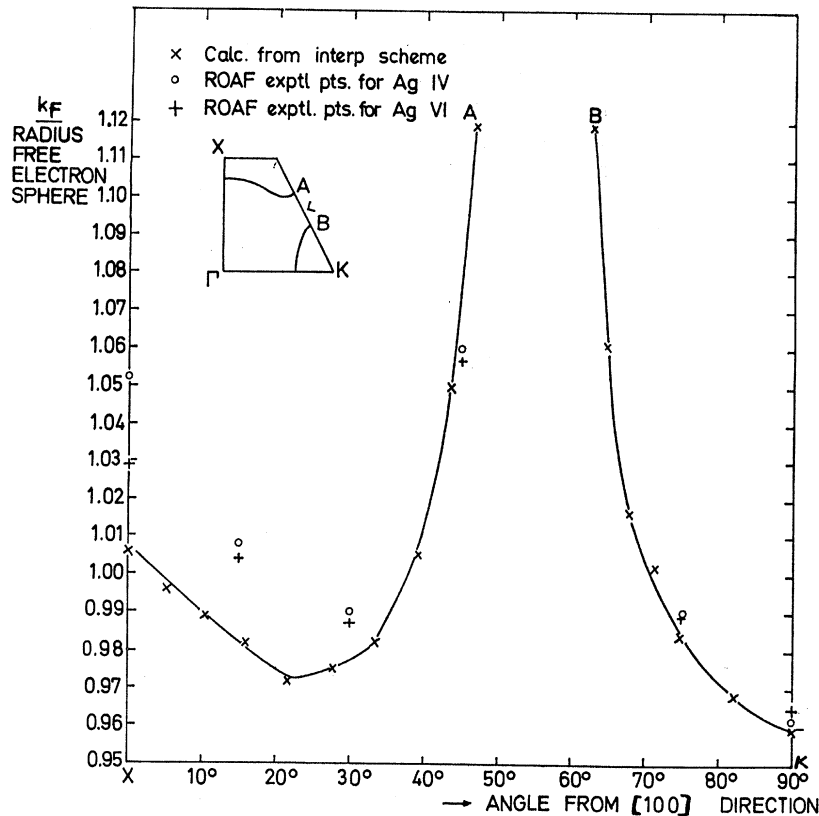


Fig. 5. Fermi radii of silver in (110) plane.

is usual to attribute such discrepancies to effects not included in the one electron approximation, e.g., electron-phonon interaction, and this is discussed later in connection with the electronic specific heats.

Also shown in Table VI are the areas in k space of these various orbits. These are compared with the areas as calculated from the de Haas-van Alphen periods quoted by Shoenberg.²¹ Here we have assumed that the neck orbit is circular but have actually integrated the area in the (110) plane where we have computed the constant energy surfaces more accurately. We would thus expect the result for the dog's bone orbit to be in best agreement with experiment and this is the case.

It should be noted that our value of $0.21m_0$ for the neck orbit is slightly lower than those determined experimentally but is still higher than the value of $0.15m_0$ calculated on the basis of a constant velocity over the Fermi surface.¹⁹ Our constant energy surfaces indicate that the velocity on the necks of the Fermi surface is smaller than on other parts of the surface, thus supporting the speculation of Howard¹⁹ that it is this decreased velocity which raises the neck effective mass. On the other hand, we do not find that the effective mass for the dog's bone orbit is larger than for the belly orbit, which Howard considered to be further evidence for a lower velocity on this orbit.

²¹ D. Shoenberg, *Phil. Mag.* **5**, 105 (1960).

However, our result for the belly orbit is rather anomalous since it does not predict many-body enhancement of comparable magnitude with that for the other orbits.

B. Optical Effective Mass

The optical effective mass m_{opt}^* is the quantity occurring in the usual expression for the frequency of plasma oscillations in a solid, viz.,

$$\omega_p^2 = 4\pi n_c e^2 / m_{opt}^*,$$

where n_c is the number of electrons per unit volume in the conduction band; m_{opt}^* can be calculated²² from

$$m_{opt}^{*-1} = \frac{1}{4\pi^3 n_c \hbar^2} \int d^3k \frac{1}{3} \nabla_k^2 E_k,$$

or, transforming to a surface integral, and using the

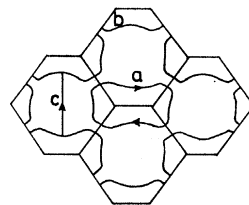


Fig. 6. Repeated zone scheme showing the three orbits considered: (a) dog's bone orbit, (b) neck orbit, and (c) central belly orbit.

²² M. H. Cohen, *Phil. Mag.* **7**, 152 (1958).

fact that $v_k = (1/\hbar)dE/dk$, we get

$$m_{\text{opt}}^{*-1} = \frac{2}{3(2\pi)^3 n_c \hbar} \int dS_f |v_k|, \quad (5.2)$$

where the integral is taken over the Fermi surface.

Since the interpolation scheme will give us the shape of constant energy surfaces in the Brillouin zone, we could thus calculate $\nabla_k E_k$ over the whole Fermi surface without too much difficulty. As an approximation, however, we can take an average value for the Fermi velocity on the belly, and following Segall,¹⁴ take the volume of the belly to be a sphere of radius \bar{k} , where

$$\bar{k} = \frac{1}{2}(k_{100} + k_{110}),$$

i.e., it is the average of the radii in the [100] and [110] directions. Segall estimates that this will lead to an error of about 5% in the belly volume, but the error should be less in silver, where there is somewhat less distortion from the free-electron sphere.

We thus integrate (5.2) separately over the belly (using the above approximations) and the eight necks, where the Fermi velocity is much smaller, using an average value for this neck velocity. We find, in this approximation,

$$m_{\text{opt}}^* = 0.95 \pm 0.05 m_0,$$

which compares reasonably well with the experimental values of Schulz²³ ($0.97 \pm 0.04 m_0$) and Ehrenreich and Philipp¹⁰ ($1.03 \pm 0.06 m_0$).

Again it is seen that the calculated value is slightly less than the experimental results, indicating perhaps some enhancement by many-body effects, though in fact our band theory result is within the range of the experimental errors.

C. Thermal Effective Mass

The thermal effective mass m_{th}^* is defined by

$$m_{\text{th}}^*/m_0 = \gamma/\gamma_0,$$

where γ/γ_0 is the ratio of the electronic specific heat of the metal to the free-electron value of this quantity for the metal. γ can be calculated from the usual expression¹⁹

$$\gamma = \frac{1}{3} \pi^2 k_B^2 N(E_F), \quad (5.3)$$

where $N(E_F)$ is the density of states at the Fermi level.

Our approach to the electronic properties gives us several alternative ways of calculating γ and hence m_{th}^* ; the most obvious approach is from the density-of-states calculation discussed in Sec. 3. This method has the disadvantage—for a noble metal like silver—that the density of states at the Fermi level is small (since the d bands are well below E_F); hence the precise value of $N(E_F)$, or rather an average value over an

estimated range of energy, is uncertain. The actual result from our density-of-states calculation is

$$m_{\text{th}}^* = 0.87 m_0,$$

which is a mean value from the two $N(E)$ calculations. As just indicated, though, too much faith cannot be placed in this result.

A better method of calculating m_{th}^* is to calculate it from a knowledge of the electron velocities over the Fermi surface.²²

From (5.3) we have

$$\frac{m_{\text{th}}^*}{m_0} = \frac{\gamma}{\gamma_0} = \frac{N(E_F)}{N(E_F)_0},$$

where $N(E_F)_0$ is the free-electron value. But in general

$$N(E_F) = \frac{2V}{(2\pi)^3} \int \frac{dS_f}{|\text{grad}_k E_k|},$$

for a volume V of specimen, where the integral is taken over the Fermi surface.

Since $v_k = (1/\hbar) \text{grad}_k E_k$, we have

$$N(E_F) = \frac{2V}{(2\pi)^3} \frac{1}{\hbar} \int \frac{dS_f}{v_k}, \quad (5.4)$$

where V_k is the Fermi velocity.

For free electrons

$$|\text{grad}_k E_k| = \frac{\hbar^2 k}{m_0},$$

while the Fermi surface is spherical with area $S_f^0 = 4\pi k_F^2$. Hence

$$n(E_F)_0 = \frac{2V}{(2\pi)^3} \frac{4\pi k_F^2}{\hbar^2 k_F / m_0}. \quad (5.5)$$

Thus from (5.4) and (5.5)

$$\frac{\gamma}{\gamma_0} = \frac{\hbar^2 k_F}{m_0} \frac{1}{4\pi k_F^2} \frac{1}{\hbar} \int \frac{dS_f}{v_k},$$

or

$$m_{\text{th}}^* = \frac{\hbar k_F}{S_f^0} \int \frac{dS_f}{v_k}. \quad (5.6)$$

The value of S_f^0 can easily be derived from the requirement that the Fermi surface enclose half the volume of the Brillouin zone, since the conduction band in silver is half full.

To carry out the integration in (5.6) we make the same assumptions as previously and integrate separately over the necks and belly of the Fermi surface. We find from our calculated Fermi surface that

$$m_{\text{th}}^* = 0.91 \pm 0.04 m_0.$$

²³ L. G. Schulz, Phil. Mag. Suppl. 6, 102 (1957).

An alternative approach is to use the expression¹⁴

$$N(E_F) = \frac{2}{(2\pi)^3} \left[\frac{\partial V_k(E)}{\partial E} \right]_{E_F},$$

where V_k is the volume enclosed by a constant energy surface.

By comparing the volume enclosed by our calculated Fermi surface with the volume of the free-electron Fermi sphere we find

$$m_{th}^* = 0.88 \pm 0.02 m_0.$$

It is likely that this result is slightly more accurate than the previous one since no assumptions about average Fermi velocities, etc., are involved. It is seen from our calculated values for the quantities that $m_{th}^* < m_{opt}^*$, which is in agreement with Cohen's result²² that this inequality should hold when the Fermi surface contacts the zone boundary.

These two calculated values, i.e., discounting our density-of-states result, which is probably fortuitous, agree within the estimated errors. These values compare with experimental results of $0.96 \pm 0.01 m_0$ by Schulz²³ and $1.00 m_0$, which has been calculated from the value for γ quoted by Montgomery *et al.*²⁴

It would appear on the basis of these results that the experimental enhancement of γ above the value calculated on band theory is about 10%. This compares with an enhancement factor of 25% estimated by Zornberg and Mueller²⁵ for copper. Montgomery suggests that this enhancement might well be smaller in the case of silver and our results would confirm this.

This question of enhancement of electronic specific heats, cyclotron effective masses, etc., above the value expected from pure band theory is an important one and it appears likely that, even in nonsuperconducting metals such as silver, it is electron-phonon interaction which is the main factor causing the effect. On this assumption work is proceeding in trying to correlate the discrepancies between our results and experiment with the perturbation theory approach to electron-phonon interaction suggested by Quinn.²⁶

²⁴ H. Montgomery, G. P. Pells, and E. M. Wray, Proc. Roy. Soc. (London) **A301**, 261 (1967).

²⁵ E. I. Zornberg and F. M. Mueller, Phys. Rev. **151**, 557 (1966).

²⁶ J. J. Quinn, in *The Fermi Surface*, edited by W. A. Harrison (John Wiley & Sons, Inc., New York, 1960), p. 58.

The present calculations on silver have been done as a preliminary to studies of alloys of the silver-palladium series. In particular, attempts are being made to predict the variation of γ with composition.²⁴ Since palladium, as a transition metal, has a much higher density of states at the Fermi level, it appears that electron-phonon interaction is much more important here than in silver. How this interaction varies in the alloys and hence to what extent the variation of γ with composition is a true measure of the variation of $n(E_F)$ is an important question which has still to be resolved, as indeed has the problem of the probable spreading of the Fermi surface from an (assumed) perfectly sharp surface in a pure metal to a much more diffuse quantity in an alloy.

DISCUSSION

We have in this paper attempted to correlate a band-structure calculation for silver with the observed electronic properties of that metal. To this end we have derived a set of parameters for the band structure which appear physically plausible.

The uniqueness of this set of parameters has not been studied; we have been more concerned with showing the consistency of various physical properties such as Fermi-surface dimensions, optical data, and effective masses with our set of energy levels.

Ideally, relativistic corrections should be included in these energy levels since silver is a moderately heavy atom and such effects are likely to be more important here than in copper. It is possible, though calculations have not yet been carried out, that including spin-orbit coupling would alter the energy levels at the point L in the zone so as to bring the calculated Fermi surface neck into better agreement with experiment. On the other hand, bulk properties such as the density of states are not likely to be much affected by this interaction, which is only of interest at symmetry points in the zone.

ACKNOWLEDGMENTS

We wish to acknowledge facilities provided by the University of Lancaster Computing Centre. One of us (P.E.L.) acknowledges receipt of a Scientific Research Council Research Studentship.